Bioorganic & Medicinal Chemistry 22 (2014) 5212–5219

Contents lists available at ScienceDirect

Bioorganic & Medicinal Chemistry

journal homepage: www.elsevier.com/locate/bmc

Hepatocyte-targeting gene delivery using a lipoplex composed of galactose-modified aromatic lipid synthesized with click chemistry

Mizuha Sakashita, Shinichi Mochizuki, Kazuo Sakurai *

Department of Chemistry and Biochemistry, The University of Kitakyushu, 1-1, Hibikino, Wakamatsu-ku, Kitakyushu, Fukuoka 808-0135, Japan

ARTICLE INFO

Article history:
Received 11 June 2014
Revised 16 July 2014
Accepted 8 August 2014
Available online 17 August 2014

Keywords:
Lipoplex
Galactose-modified lipid
Gene delivery

ABSTRACT

Highly efficient drug carriers targeting hepatocyte is needed for treatment for liver diseases such as liver cirrhosis and virus infections. Galactose or *N*-acetylgalactosamine is known to be recognized and incorporated into the cells through asialoglycoprotein receptor (ASGPR) that is exclusively expressed on hepatocyte and hepatoma. In this study, we synthesized a galactose-modified lipid with aromatic ring with click chemistry. To make a complex with DNA, termed 'lipoplex', we prepared a binary micelle composed of cationic lipid; dioleoyltrimethylammoniumpropane (DOTAP) and galactose-modified lipid (D/Gal). We prepared lipoplex from plasmid DNA (pDNA) and D/Gal and examined the cell specificity and transfection efficiency. The lipoplex was able to interact with ASGPR immobilized on gold substrate in the quartz-crystal microbalance (QCM) sensor cell. The lipoplex induced high gene expression to HepG2 cells, a human hepatocellular carcinoma cell line, but not to A549 cells, a human alveolar adenocarcinoma cell line. The treatment with asialofetuin, which is a ligand for ASGPR and would work as a competitive inhibitor, before addition of the lipoplexes decreased the expression to HepG2 cells. These results indicate that D/Gal lipoplex was incorporated into HepG2 cells preferentially through ASGPR and the uptake was caused by galactose specific receptor. This delivery system to hepatocytes may overcome the problems for gene therapy and be used for treatment of hepatitis and hepatic cirrhosis.

1. Introduction

The development of an efficient gene delivery system is a primary requirement for clinical applications of gene therapies. Nonpathogenic viral vectors such as retroviruses and lentiviruses are mainly used because of their high transfection efficiency. However, their use incurs some serious problems such as potential mutagenicity, high manufacturing costs, and safety risks owing to their inflammatory effects. These issues have prompted the development of nonviral alternatives including synthetic gene carriers.[1] The most commonly used synthetic gene carriers are cationic lipids and polymers, which can form complexes with negatively charged plasmid DNA (pDNA) via electrostatic interactions. Although several cationic compounds have been investigated, many issues must be resolved before they can be used in human therapy. One of the most pressing problems is a lack of cellular selectivity, which results in low uptake efficiency into the target cells. Various chemical modifications have been used to overcome this obstacle. For example, ligand molecules that promote the accumulation of therapeutic agents in the target cells are attached to the gene carriers. Sugars are ligands that can be used for receptor-targeted delivery, such as galactose for hepatocytes,[2–4] hyaluronic acid for liver sinusoidal endothelial cells,[5,6] and mannose for macrophages.[7,8]

Therapy for liver diseases including cirrhosis and viral infections is one of the most critical health challenges worldwide because of a lack of fundamental treatments besides resection and transplantation. Hepatocytes, the liver parenchymal cells, constitute the majority of liver tissue and are mainly affected in liver diseases. Asialoglycoprotein receptor (ASGPR) is exclusively expressed on hepatocytes;[9] it recognizes asialoglycoproteins that contain terminal galactose and *N*-acetylgalactosamine residues, and internalizes them.[10,11] Several studies have focused on galactose residues as a pilot molecule for targeting hepatocytes.

We previously reported a series of lipids with an aromatic linker connected with amine or amidine that can be used as transfection reagents with better efficiency and lower cytotoxicity than conventional reagents.[12,13] Analysis of the hydrophobic moieties that induce high transfection efficiency by altering alkyl chain lengths and positions revealed that lipids with an amino residue attached

* Corresponding author. Tel.: +81 93 695 3298; fax: +81 93 695 3390.
E-mail address: sakurai@kitakyu-u.ac.jp (K. Sakurai).

http://dx.doi.org/10.1016/j.bmc.2014.08.012
0968-0896/

to C12 in the meta-meta position exhibit the highest efficiencies.[13] In addition, lipids can form stable micelles at low concentrations as a result of hydrophobic interactions among aromatic rings and 2 alkyl chains as well as π–π stacking derived from aromatic rings. The advantages of using the aromatic linker have been described in our previous papers.[12–14] Furthermore, these lipids are easy to synthesize with high yield by using click chemistry.

In this study, we synthesized galactose-modified lipids with an aromatic ring with C12 in the meta-meta position. The galactose-modified lipids were mixed with cationic lipids to form complexes with DNA, which are termed 'lipoplexes'. We subsequently investigated their transfection efficiencies into cells expressing ASGPR.

2. Materials and methods

2.1. Materials

3,5-Dihydroxybenzaldehyde, potassium carbonate, propargylbromide, sodium L-ascorbic acid, Dulbecco's modified Eagle's medium (DMEM) were purchased from Wako Pure Chemical Industries, Ltd, (Osaka, Japan). 1-Bromododecane, sodium boronhydride, sodium hydride were purchased from Tokyo Chemical Industry Co., (Tokyo, Japan). *N*-*N*-dimethlformamide, sodium methoxide were purchased from Kanto Chemical Co., (Tokyo, Japan). 1-azido-1-deoxy-β-D-galactopyranoside acetate, copper(II) sulfate pentahydrate were purchased from Sigma–Aldrich (St. Louis, MO).

2.2. Synthesis of the sugar-modified lipid (Scheme 1)

3,5-Dihydroxybenzaldehyde, 1-bromododecane and potassium carbonate was mixed in *N*,*N*-dimethylformamide at molar ratio of 1:2:5 and stirred at 80 °C for 6 h. The reaction mixture was extracted with ethyl acetate and purified compound **I** by silica gel chromatography using a mixture of hexane and dichloromethane (hexane/dichloromethane = 1:1) as a mobile phase. The compound **I** and sodium boronhydride were mixed in solution of methanol and tetrahydrofuran (methanol/tetrahydrofuran = 5: 1) at molar ratio of 1: 2 and stirred at rt for 2 h under a nitrogen atmosphere. The reactant was added dichloromethane and 1 N hydrogen chloride for neutralization. We extracted the organic phase and purified compound **II** by silica gel chromatography using dichloromethane. The compound **II**, propargylbromide and sodium hydride were mixed in *N*,*N*-dimethylformamide at molar ratio of 1:3:11 and stirred at rt for 19 h under a nitrogen atmosphere. The reactant was extracted with ethyl acetate and purified compound **III** by silica gel chromatography using a mixture of hexane and dichloromethane (hexane/dichloromethane = 1:1). The compound **III**, 1-azido-1-deoxy-β-D-galactopyranoside acetate, sodium L-ascorbic acid and copper(II) sulfate pentahydrate were added in *N*,*N*-dimethylformamide at molar ratio of 1:1:1:0.07 and stirred at 90 °C for 16 h. The reactant was extracted with ethyl acetate and purified compound **IV** by silica gel chromatography using a mixture of ethyl acetate and hexane (ethyl acetate/hexane = 2:3). The compound **IV** and sodium methoxide was mixed in methanol at molar ratio of 1:0.6 and stirred at rt for 4 h under a nitrogen atmosphere. The reactant was added 6 N hydrogen chloride for neutralization and centrifuged at 300×*g* for 20 min. We collected the organic phase and obtained compound **V** with evaporation. The obtained galactose modified lipid was identified by ^{1}H NMR. δ_H (500 MHz, methanol-d_4): δ = 8.23 (1H, s, CH), 6.50 (2H, s, ArH), 6.36 (1H, s, ArH), 5.58 (1H, d, J = 9.4 Hz, 1-CH), 4.64 (2H, s, OCH_2), 4.50 (2H, s, OCH_2), 4.14 (1H, t, J = 9.4 Hz, 3-CH), 3.98 (1H, d, J = 3.0 Hz, 2-CH), 3.93 (5H, t, 4-CH and 2 × OCH_2), 3.85–3.68 (3H, m, 5-CH and 6-CH_2), 1.77–1.71 (4H, m, 2 × OCH_2CH_2), 1.49–1.43 (4H, m, 2 × CH_2CH_3), 1.38–1.29 (32H, m, 2 × C_8H_{16}), 0.91–0.88 (6H, t, J = 6.9 Hz, 2 × CH_3). FAB-MS (m/z): $[M+Na]^+$ calcd for $C_{40}H_{69}N_3O_8Na$ 742.69; found 742.98. We obtained the glucose modified lipid in the same way using 1-azido-1-deoxy-β-D-glucopyranoside.

2.3. Preparation of the lipoplex composed of sugar-modified lipid/cationic lipid micelle and plasmid DNA

We mixed the sugar-modified lipid and dioleoyltrimethylammoniumpropane (DOTAP; Sigma–Aldrich) at the same molar ratio and dissolved them in chloroform and vacuum dried. Each mixture was dissolved in water and added the pDNA encoding luciferase (pGL3-Control Vector; Promega, Madison, WI) at the indicated N/P ratios (i.e., the cation/anion charge ratio, $[\text{cationic amino group}]_{DOTAP}/[\text{anionic phosphate group}]_{\text{nucleic acid}}$) and incubated for 1 h. To confirm the complexations, the mixtures were separated by 1% agarose gel electrophoresis. DNA was stained with ethidium bromide and the image was obtained using a PharosFX (Bio-Rad, Richmond, CA).

2.4. ζ Potential and size measurements

We prepared the lipoplexes at indicated N/P ratios in 150 mM NaClaq, where we fixed DOTAP concentration at 0.3 mM. The zeta potentials and hydrodynamic radiuses were measured with a Malvern Zetasizer nano (Malvern Instruments, Malvern, UK) at room temperature.

2.5. Small-angle X-ray scattering (SAXS) measurement

SAXS measurements from the D/Gal and D/Glc lipoplex were carried out at BL40B2 SPring-8 with a 0.7 m camera using a Rigaku imaging plate (30 × 30 cm, 3000 × 3000 pixels) as a detector. The wavelength of the beam was 0.71 Å, and the exposure time was 300 s. The obtained two dimensional image was circularly averaged to give an intensity $I(q)$ versus q plots, where q is the magnitude of the scattering vector defined by $q = 4\pi\sin\theta/\lambda$ with the scattering angle of 2θ. The concentration of sugar-modified lipids was 6 mM.

2.6. Interaction between ASGPR and lipoplexes

The anti-His6 antibody (Thermo SCIENTIFIC, Waltham, MA) was immobilized on gold substrate in the quartz-crystal microbalance (QCM) sensor cell (AFFINIX QNμ; INITIUM, Inc., Tokyo, Japan) for 1 h at rt After blocking with 1% BSA in PBS for 1 h, ASGPR (R&D Systems, Inc., Minneapolis, MN) in PBS was added into the sensor cell at 25 μg/ml and incubated for 1 h at rt After washing with PBS three times, the sensor cell was filled with 500 μl of 10 mM Tris–HCl containing 2 mM $CaCl_2$ and 0.1% BSA and added the samples at 4 μg/ml and measured the frequency changes at 25 °C.

2.7. Gene transfection

HepG2 or A549 cells were seeded at 1.0×10^4 cells in a collagen-coated 96-well microplate and incubated at 37 °C under 5% CO_2. The cells were cultured in DMEM containing 10% FBS and 100 U/ml penicillin, and 0.1 mg/ml streptomycin. After 24 h, the cells were transfected with the pDNA at 0.2 μg/ml using the lipoplexes or Lipofectamine 2000 (invitrogen, Carlsbad, CA). In brief, on the day of transfection, the wells were replaced with fresh medium without serum and added the lipoplexes at the indicated N/P ratio. After 6 h, the wells were replaced with fresh medium containing serum. After 48 h, the cells were washed with PBS twice adequately and then lysed with a lysis buffer from the luciferase

assay kit (Promega). After adding of luciferin, the luciferase activity in an aliquot of the cell lysate was measured with a luminescence plate reader (Wallac 1420; Perkin Elmer, Wellesley, MA). The protein concentration of each well lysate was determined by a standard protein assay (Dojindo, Kumamoto, Japan). The luciferase activity in each sample was normalized to the luminescence intensity per microgram of protein.

2.8. Uptake of lipoplexes into the cell

HepG2 cells were seeded at 1.0×10^4 cells in 96-well microplate, and incubated for 24 h. After washed with DMEM, the cells were transfected with the FITC-labeled pDNA at 2 μg/ml using the lipoplex in serum free medium. 1, 3 or 6 h later, we washed the cells with PBS twice and observed the fluorescence image using a BZ-9000 digital fluorescence microscope (Keyence, Osaka, Japan). FITC-labeled pDNA was prepared using Label IT *R* Fluorescein Labeling Kit (Mirus Bio LLC., Madison, WI).

3. Results

3.1. Preparation and characterization of lipoplexes

As the prepared galactose- and glucose-modified lipids (Scheme 1) have no cationic charge, they are unable to form a complex with pDNA encoding luciferase via electrostatic interactions. In addition, the sugar-modified lipids themselves are unable to form micelles owing to their low solubility. In this study, we added the cationic lipid DOTAP to the sugar-modified lipids to obtain micelles. We presumed that positively charged DOTAP can uniformly mix with the sugar lipid, conferring solubility and the ability to bind DNA. To avoid nonspecific cellular uptake due to DOTAP, it was preferable to use a DOTAP composition as low as possible. We determined the lowest DOTAP composition capable of forming stable micelles to be a 1:1 molar mixing ratio. Herein, we denote the galactose- and glucose-modified micelles as D/Gal and D/Glc, respectively. After mixing pDNA with D/Gal, D/Glc or DOTAP at an appropriate N/P ratio, lipoplex formation was examined by agarose gel electrophoresis (Fig. 1). For DOTAP, no free DNA bands were observed at N/P >2. The same results were obtained for the mixtures of pDNA with D/Gal and D/Glc micelles, indicating that the addition of D/Glc (or D/Gal) does not obstruct lipoplex formation. Therefore, D/Gal, and D/Glc can form stable lipoplexes at N/P >2.

The ζ potentials and hydrodynamic radii of the resultant lipoplexes were measured at various N/P ratios (Fig. 2A, S1 and Table S1). For all samples, the ζ potentials changed from negative to positive charge at N/P = 2 with increasing N/P (Fig. 2A). The hydrodynamic radii also increased drastically with increasing N/P ratio, reaching 3–5 μm around N/P = 2. This maximum occurred because the surface charges were cancelled by pDNA, resulting in the formation of large aggregates. After the maximum appeared, the hydrodynamic radii decreased with increasing N/P ratio, reaching approximately 100 nm at N/P >5 (Fig. S1). This result indicates that the extra cationic lipids dissolved the aggregation and dispersed the complex uniformly.

At N/P >2, the ζ potentials increased slowly, plateauing at N/P = 5. The ζ potentials of D/Gal and D/Glc lipoplexes were lower than that of DOTAP lipoplexes despite the same concentration of DOTAP. The ζ potential is related to the electrical charge at the interface between a solid surface and its liquid medium and does not reflect the total charge of the entire particle.[15] Thus these results suggest that both lipoplexes containing sugar-modified lipids express the sugar residues on the surface, resulting in low ζ potentials.

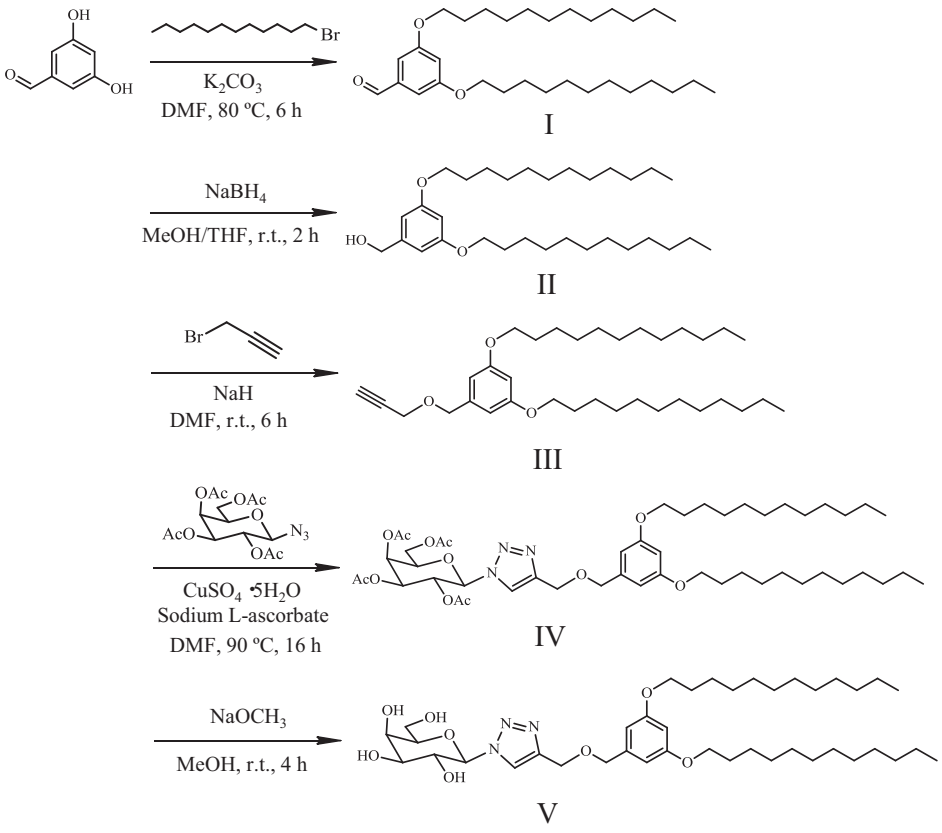

Scheme 1. Synthetic route of galactose-modified lipid through click chemistry.

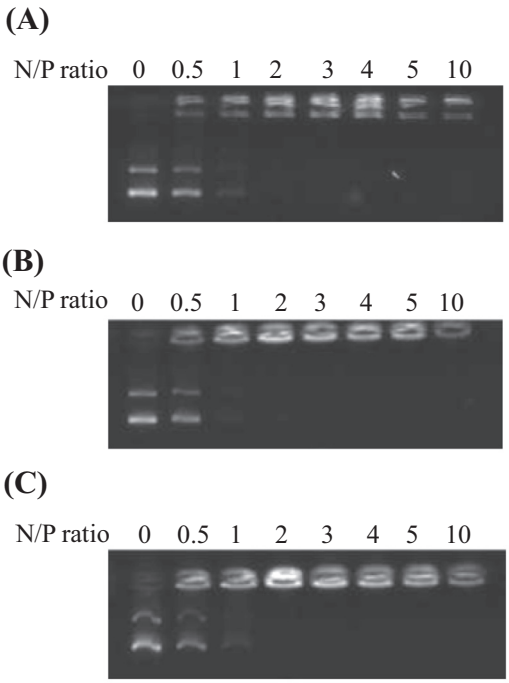

Figure 1. Confirmation of the complexation between pDNA and D/Gal (A), D/Glc (B) or DOTAP (C) at indicated N/P ratios.

By using SAXS, Safinya and co-workers proposed the relationship between the supramolecular structure of lipoplexes and their transfection efficiency.[16–18] They state that most cationic lipids undergo structural transition with the addition of DNA and some of them are catabolized into hexagonally packed cylinders including inverted hexagonal[17] and DNA/tubular-lipid intercalated[18] structures. We examined the structures of D/Gal and D/Glc lipoplexes using SAXS (Fig. 2B). Both lipoplexes exhibited sharp diffraction peaks, indicating the formation of ordered structures. As the positions satisfied the relation of 1: $\sqrt{3}$:2:$\sqrt{7}$, this indicates that the lipoplexes formed a hexagonally packed cylindrical structure (Fig. S2A).[19] The inter-cylinder distances determined from the peak positions were almost the same for both lipoplexes. The results collectively indicate that D/Gal and D/Glc lipoplexes have the same characteristics including particle size, surface charge, and inner structure. We measured SAXS profile changes upon mixing D/Gal and DNA (Fig. S2B). D/Gal lipid exhibited characteristic peaks ascribed to hexagonally packed cylinders, indicating the entanglement of tubular lipids. The addition of DNA did not alter hexagonal packing, but the peak positions were shifted to higher angles. This result indicates that negatively charged DNA reduces or cancels electrostatic repulsions between the adjoining tubular lipids by intercalating with each other. This implies that D/Gal lipoplexes adopt a DNA/tubular-lipid intercalated packing. Moreover, assuming that the bound DNA in the DNA/tubular-lipid intercalated packing takes a different order from the lipids, this structure may explain the presence of the additional peak at q = 1.13 nm^{-1}. Nevertheless, a more detailed structural analysis technique such as anomalous X-ray scattering is required to identify where the bound DNA is located in the lipoplexes.

We measured the critical micellar concentration (CMC) for D/Gal and D/Glc lipids by using fluorescence probe 8-anilino-1-naphthalene sulfonic acid (ANS).[14] Both lipids exhibited 70 nM (Fig. S3), which is considerably lower than those of other cationic lipids used for DNA transfection.

In summary, in the range of N/P >4, in which we performed the main biological assays, D/Gal and D/Glc lipoplexes formed presumably spherical nanoparticles <100 nm. The particles were positively charged and the tubular lipids and DNA were hexagonally packed within the particles.

3.2. Gene expression efficiency

In order to optimize transfection efficiency, the gene expression of the lipoplexes was evaluated in HepG2 cells, a human hepatocellular carcinoma cell line with strong ASGPR surface expression, at

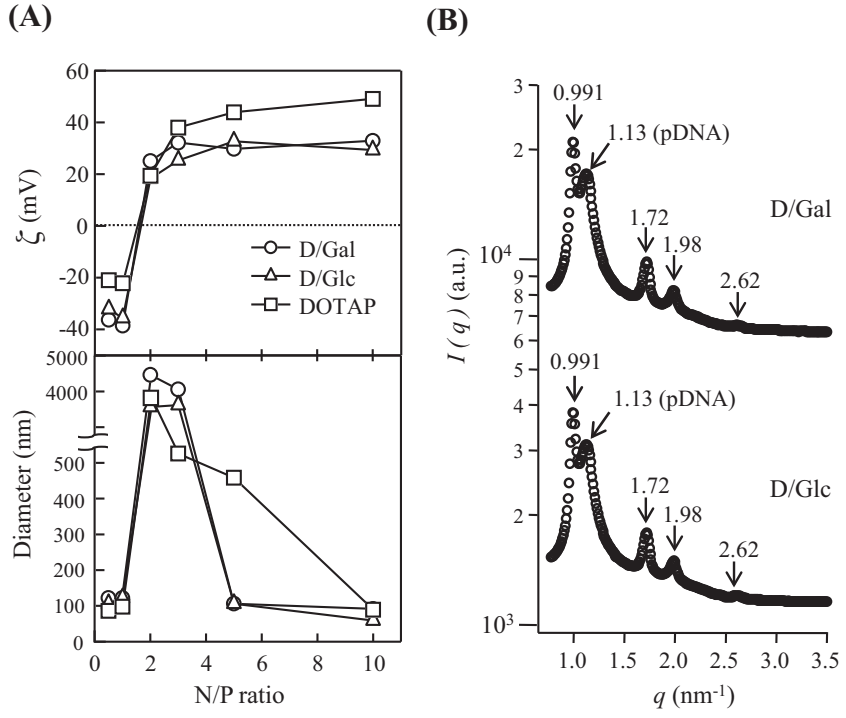

Figure 2. Characterization of the lipoplexes determined with dynamic light scattering measurements (A) and SAXS profiles at N/P = 5 (B).

N/P = 3, 5, and 10 (Fig. 3). As mentioned above, inadequate complexation and precipitation were observed at N/P <2. Therefore, we focused on N/P ratios of 3, 5, and 10. Relatively high gene expression was observed for D/Gal lipoplexes. Meanwhile, D/Glc and DOTAP lipoplexes hardly induced gene expression at any N/P ratio. These results suggest that D/Gal lipoplexes can induce gene expression with the aid of a galactose-modified lipid. The highest efficiency among the D/Gal samples occurred at N/P = 5; notably, the expression level was 3-fold higher than that for Lipofectamine 2000. The reason for the observed N/P dependence of the efficiency can be explained as follows. At N/P <5, some lipoplexes are thought to aggregate and make large particles (Fig. 2A), impeding cellular uptake and resulting in low gene expression. At N/P >5, the lipoplexes exhibit strong cytotoxicity because of their excessive cationic lipids (Fig. S4). Accordingly, as D/Gal lipoplexes induced the highest gene expression efficiency at N/P = 5, we evaluated the following examinations at N/P = 5 hereafter.

3.3. Lipoplex uptake into HepG2 cells

In order to achieve efficient gene expression, the pDNA carrier must satisfy the following requirements: (1) cellular uptake, (2) endosomal escape, and (3) nuclear transfer. Here, we investigated the cellular uptake of the lipoplexes using FITC-labeled pDNA. Figure 4A shows fluorescent images at the indicated times after adding the lipoplexes to HepG2 cells. D/Gal and DOTAP lipoplexes were incorporated into the cells in a time-dependent manner. As expected, the cells treated with D/Gal lipoplexes exhibited the strongest fluorescence at all time points. The fluorescence intensity for the cells treated with D/Gal lipoplexes at 6 h was 5-fold greater than that of cells treated with DOTAP lipoplexes (Fig. 4B). When D/Gal lipoplexes were added to A549 cells, a human alveolar adenocarcinoma cell line, no fluorescence was observed in the cells (Fig. S5). These results indicate that the galactose-modified lipid promotes specific cellular uptake for hepatomas. Meanwhile, the cellular fluorescence at 1 hour in cells treated with D/Glc lipoplexes was the same as that of cells treated with D/Gal lipoplexes. Huge fluorescent precipitates larger than the cells were observed at 3 and 6 h; these precipitates that forms with D/Glc lipoplexes may be due to cellular interactions with HepG2 cells. In fact, no precipitates on A549 cells were observed when D/Glc lipoplexes were added to the cells (Fig. S5). As cellular uptake is the essential factor for efficient gene expression in the present system, D/Gal lipoplexes exhibited the highest gene expression.

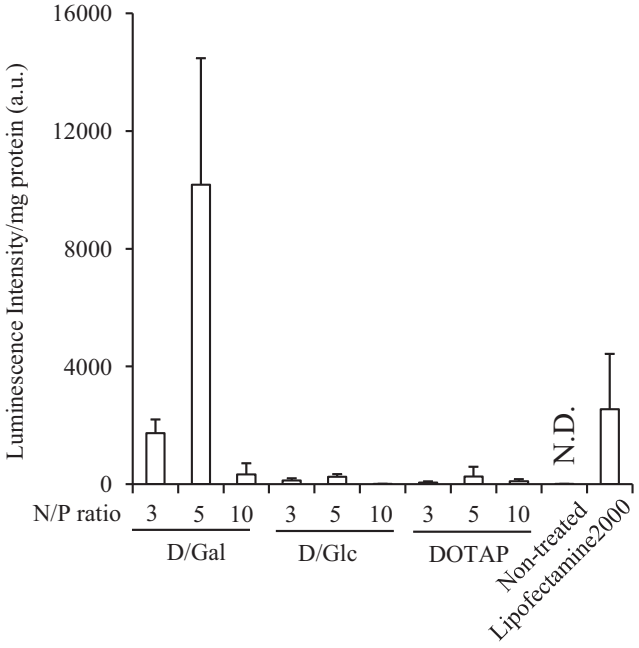

Figure 3. Transfection efficiencies for the lipoplexes at indicated N/P ratios. N.D.; not detected. Data represent the mean ± SD of triplicate wells.

3.4. Binding of D/Gal lipoplexes to ASGPR

Uptake into HepG2 cells is considered to be due to the interaction between ASGPR and the galactose-modified lipids within lipoplexes. Accordingly, we examined the binding of D/Gal to ASGPR by QCM, which measures the decrease in the frequency of a quartz crystal immersed in solutions, which is directly related to the increase in mass due to the surface adsorption of guest molecules onto the resonator. Figure 5A shows the QCM frequency changes when equal masses of D/Gal, D/Glc, or DOTAP were added into the QCM cell. The addition of D/Gal rapidly decreased the frequency, whereas D/Glc and DOTAP did not. The same results were observed even after complexation with pDNA (Fig. 5B). These results indicate that the galactose moiety in D/Gal micelles is exposed to the surface irrespective of complexation with pDNA and can bind to ASGPR. This also corroborates the results of the high transfection efficiency and uptake of D/Gal lipoplexes into HepG2 cells (Figs. 3 and 4).

3.5. Gene expression induced by ASGPR-mediated uptake

We examined the gene expression efficiency in cells with and without ASGPR. The A549 cells do not express ASGPR on their surface. D/Gal lipoplexes induced higher gene expression than Lipofectamine 2000 in HepG2 cells but not A549 cells (Fig. 6A). Meanwhile, D/Glc and DOTAP lipoplexes did not exhibit high gene expression in either cell line. When HepG2 cells were pretreated with asialofetuin, which possesses 3 *N*-linked triantennary chains with 9 terminal *N*-acetyllactosamine residues,[9,20] before adding the lipoplexes, the gene expression of the cells treated with D/Gal lipoplexes decreased drastically (Fig. 6B). The expressions induced by D/Glc, DOTAP, and Lipofectamine 2000 lipoplexes did not differ regardless of asialofetuin treatment. These results indicate that D/Gal lipoplexes induce high preferential gene expression in cells expressing galactose-specific receptors.

4. Discussion

Various synthetic carriers containing galactose-modified cationic lipids and polymers for delivering molecules to hepatocytes have been developed. ASGPR is a C-type lectin that plays a role in the clearance of desialylated serum proteins such as fibronectin[21] and all IgA2 allotypes.[22] The carbohydrate recognition domain of ASPGR can bind at least a single-terminal galactose or galactosamine residue. The affinity of ligands for ASGPR increases with the valence of sugar residues. Lee et al. demonstrated that multivalent glycosides bind to receptors simultaneously, enhancing affinity compared to monovalent glycosides.[23,24] This phenomenon is known as the 'cluster effect'. The cluster effect can be induced by only 3 galactose residues and does not require a large molecular size. In addition, the distance between galactose residues plays a significant role in this effect; the appropriate spacing for the receptor recognition of cluster glycosides is determined to be 15–25 Å.[24,25]

In the present study, the lipoplexes with galactose-modified lipids specifically delivered pDNA into hepatoma cells with high transfection efficiency. Furthermore, the observations of cellular uptake (Fig. 4) and binding to ASGPR (Fig. 5) indicate that the

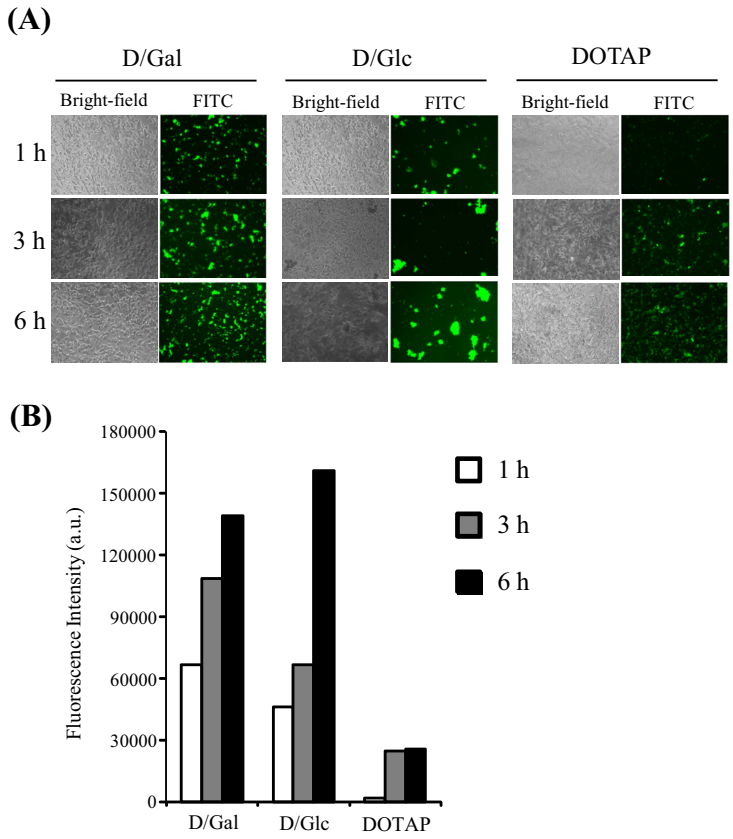

Figure 4. Uptake of the lipoplexes to HepG2 cells. After treatment with the lipoplexes for 1, 3 or 6 h at N/P ratio = 5, the cells were observed with a fluorescence microscopy (A) and measured the fluorescence intensities (B).

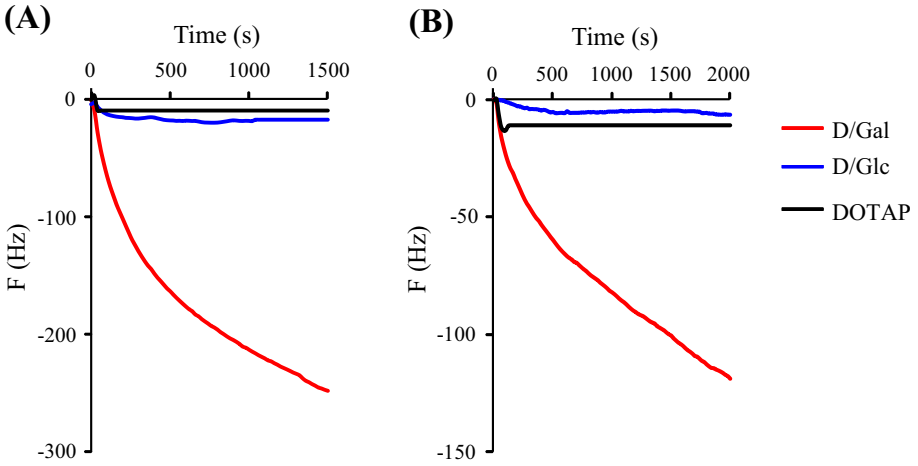

Figure 5. Time courses of frequency changes of ASGPR immobilized QCM in response to addition of D/Gal (red line), D/Glc (blue line) and DOTAP (black line) before (A) and after (B) complexation with pDNA (N/P = 5).

galactose residues can be exposed to the surface of lipoplexes. These results suggest that the distances between galactose residues on the prepared lipoplexes are optimal; this distance is considered to be governed by the galactose-modified lipid content in D/Gal micelles and can be easily controlled by changing the mixing ratio between galactose-modified lipids and DOTAP. Therefore, it is possible to optimize lipoplexes for high transfection efficiency into hepatocytes if the galactose residues on the lipoplexes can be precisely located. When the galactose-modified lipid content is low, the distance between galactose residues may become too large to bind to the receptor. In contrast, when the galactose content is high, receptor recognition can be enhanced. The N/P ratio is another factor that determines the transfection efficiency. Although D/Gal lipoplexes exhibited almost the same ζ potentials and hydrodynamic radii at N/P ratios of 5 and 10 (Fig. 2), the transfection efficiency was much higher at 5 than 10 (Fig. 3). In addition to the high cytotoxicity described above, at N/P = 10, free D/Gal micelles can exist because of excessive feed, resulting in the competitive inhibition of the binding of D/Gal lipoplexes to ASGPR on HepG2 cells. The difference in cytotoxicity between N/P ratio of 5

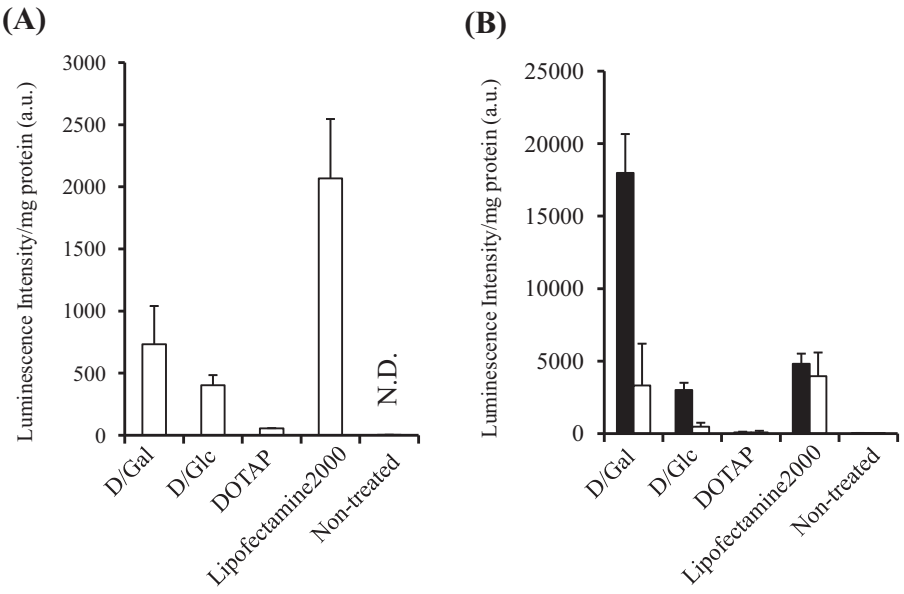

Figure 6. Gene expression through galactose specific receptor. (A) Transfection efficiencies for the lipoplexes to A549 cells at N/P ratio = 5. N.D.; not detected. (B) After HepG2 cells were treated with (white bar) or without (black bar) asialofetuin at 1 mg/ml for 1 h, the transfection efficiencies by the lipoplexes were measured at N/P ratio = 5. Data represent the mean ± SD of triplicate wells.

and 10 (Fig. S4) suggests that the low gene expression at an N/P ratio of 10 is attributable to the latter cause.

In general, pDNA needs to escape from endosomal compartments for gene expression after uptake into cells. Therefore, in order to increase transfection efficiency, a neutral phospholipid such as L-α-dioleoylphosphatidylethanolamine (DOPE) or L-α-dilauroylphosphatidylcholine (DLPC) is added to cationic lipids as a helper co-lipid.[26–28] In particular, DOPE is a phospholipid that undergoes structural transition with pH change and induces interaction with endosomal vesicles; thus, it can release bound DNA or escape into the cytosol.[29,30] In fact, DOTAP lipoplexes hardly induced gene expression in the present study, although lipoplex uptake into HepG2 and A549 cells was observed. However, after forming micelles with sugar-modified lipids, D/Gal and D/Glc lipoplexes induced slight gene expression in A549 cells. As A549 cells have no ASGPR or receptors to uptake glucose via endocytosis, the uptake into the cells was caused by DOTAP in a nonspecific manner. This suggests sugar-modified lipids facilitate gene expression in cells. The present results confirm both D/Gal and D/Glc lipoplexes form hexagonally packed cylindrical structures at pH 7.0 (Fig. 2B). The sugar-modified lipids have a triazole ring as a functional group in response to pH changes. As the pK_a of triazole rings is 4.0–5.0,[31] some sugar-modified lipids can be assumed to undergo structural transition in response to endosomal pH (pH 5.0–6.0). Such partial structural transition may induce overall structural transition of the lipoplexes, causing them to interact with endosomal components in cells, consequently facilitating gene expression. Another reason for endosomal escape is the alkyl chains of galactose-modified lipids. Alkyl chain length and position are reported to affect cellular membrane destabilization.[32,33] Therefore the alkyl chains of the prepared lipids may be suitable for destabilizing the endosomal membrane. Nevertheless, the precise roles of the sugar-modified lipids in cells and intracellular behaviors require further investigation.

Another issue to be overcome in the design of highly efficient drug delivery system (DDS) nanoparticles is providing appropriate stability to lipoplexes. After in vivo administration, the concentration of DDS nanoparticles decrease to below the nanomolar level; moreover, the nanoparticles may interact with and be inactivated by many other components such as proteins in biological fluids. To maintain particle structures in such conditions, the critical micellar concentration must be low and the interactions that construct the micellar structures must be strong enough such that other components do not interfere. One of the essential driving forces to form lipoplexes is electrostatic interactions arising from the ion-pairs between DNA and cationic head groups and the hydrophobicity of the lipids. The present study demonstrated that the lipids with an aromatic linker between alkyl tails and head groups are more hydrophobic than conventional lipids that have been used for DDS (Table S2).[14] CMC of D/Gal was determined to be 70 nM (Fig. S3), which is also quite low, suggesting that the micellar stability owing to its high hydrophobicity is a huge advantage for in vivo study.

In conclusion, lipoplexes comprising equimolar amounts of pDNA and D/Gal exhibited good transfection efficiency at N/P = 5. Although D/Gal and D/Glc lipoplexes do not differ with respect to size, surface charge, or supramolecular structure, they distinctly differ with respect to ASGPR recognition and gene expression. D/Gal lipoplexes bound to ASGPR were immobilized on the QCM sensor cell and exhibited ASGPR-dependent gene expression. Therefore, the present study suggests our lipoplexes with galactose residues can be used to treat hepatitis and hepatic cirrhosis.

Acknowledgments

All SAXS measurements were carried out at SPring-8 40B2 (2011A1668 and 2011B1468).

Supplementary data

Supplementary data associated with this article can be found, in the online version, at http://dx.doi.org/10.1016/j.bmc.2014.08.012.

References and notes

1. Kawakami, S.; Higuchi, Y.; Hashida, M. *J. Pharm. Sci.* **2008**, *97*, 726.
2. Wu, G. Y.; Wu, C. H. *J. Biol. Chem.* **1987**, *262*, 4429.
3. Hashimoto, M.; Morimoto, M.; Saimoto, H.; Shigemasa, Y.; Sato, T. *Bioconjug. Chem.* **2006**, *17*, 309.

4. Perales, J. C.; Grossmann, G. A.; Molas, M.; Liu, G.; Ferkol, T.; Harpst, J.; Oda, H.; Hanson, R. W. *J. Biol. Chem.* **1997**, *272*, 7398.
5. Asayama, S.; Nogawa, M.; Takei, Y.; Akaike, T.; Maruyama, A. *Bioconjug. Chem.* **1998**, *9*, 476.
6. Takei, Y.; Maruyama, A.; Ferdous, A.; Nishimura, Y.; Kawano, S.; Ikejima, K.; Okumura, S.; Asayama, S.; Nogawa, M.; Hashimoto, M.; Makino, Y.; Kinoshita, M.; Watanabe, S.; Akaike, T.; Lemasters, J. J.; Sato, N. *FASEB J.* **2004**, *18*, 699.
7. Hashimoto, M.; Morimoto, M.; Saimoto, H.; Shigemasa, Y.; Yanagie, H.; Eriguchi, M.; Sato, T. *Biotechnol. Lett.* **2006**, *28*, 815.
8. Un, K.; Kawakami, S.; Yoshida, M.; Higuchi, Y.; Suzuki, R.; Maruyama, K.; Yamashita, F.; Hashida, M. *Biomaterials* **2011**, *32*, 4659.
9. Ashwell, G.; Harford, J. *Annu. Rev. Biochem.* **1982**, *51*, 531.
10. Spiess, M. *Biochemistry* **1990**, *29*, 10009.
11. Geffen, I.; Spiess, M. *Int. Rev. Cytol.* **1992**, *137B*, 181.
12. Koiwai, K.; Tokuhisa, K.; Karinaga, R.; Kudo, Y.; Kusuki, S.; Takeda, Y.; Sakurai, K. *Bioconjug. Chem.* **2005**, *16*, 1349.
13. Mochizuki, S.; Kamikawa, Y.; Nishina, K.; Fujii, S.; Hamada, E.; Kusuki, S.; Matsuo, T.; Sakurai, K. *Bull. Chem. Soc. Jpn.* **2012**, *85*, 354.
14. Nishimura, T.; Cho, T.; Kelley, A. M.; Powell, M. E.; Fossey, J. S.; Bull, S. D.; James, T. D.; Masunaga, H.; Akiba, I.; Sakurai, K. *Bull. Chem. Soc. Jpn.* **2010**, *83*, 1010.
15. Delgado, A. V.; Gonzalez-Caballero, F.; Hunter, R. J.; Koopal, L. K.; Lyklema, J. *J. Colloid Interface Sci.* **2007**, *309*, 194.
16. Ewert, K.; Slack, N. L.; Ahmad, A.; Evans, H. M.; Lin, A. J.; Samuel, C. E.; Safinya, C. R. *Curr. Med. Chem.* **2004**, *11*, 133.
17. Koltover, I.; Salditt, T.; Radler, J. O.; Safinya, C. R. *Science* **1998**, *281*, 78.
18. Ewert, K. K.; Evans, H. M.; Zidovska, A.; Bouxsein, N. F.; Ahmad, A.; Safinya, C. R. *J. Am. Chem. Soc.* **2006**, *128*, 3998.
19. Fengji, Y.; Eugene, L. S.; Alexei, R. K.; Benjamin, C. *J. Am. Chem. Soc.* **1996**, *118*, 6615.
20. Tolleshaug, H.; Berg, T. *Hoppe. Seylers. Z. Physiol. Chem.* **1980**, *361*, 1155.
21. Rotundo, R. F.; Rebres, R. A.; McKeown-Longo, P. J.; Blumenstock, F. A.; Saba, T. M. *Hepatology* **1998**, *28*, 475.
22. Rifai, A.; Fadden, K.; Morrison, S. L.; Chintalacharuvu, K. R. *J. Exp. Med.* **2000**, *191*, 2171.
23. Lee, Y. C.; Townsend, R. R.; Hardy, M. R.; Lonngren, J.; Arnarp, J.; Haraldsson, M.; Lonn, H. *J. Biol. Chem.* **1983**, *258*, 199.
24. Lee, R. T.; Lin, P.; Lee, Y. C. *Biochemistry* **1984**, *23*, 4255.
25. Biessen, E. A.; Beuting, D. M.; Roelen, H. C.; van de Marel, G. A.; van Boom, J. H.; van Berkel, T. J. *J. Med. Chem.* **1995**, *38*, 1538.
26. Felgner, P. L.; Gadek, T. R.; Holm, M.; Roman, R.; Chan, H. W.; Wenz, M.; Northrop, J. P.; Ringold, G. M.; Danielsen, M. *Proc. Natl. Acad. Sci. U.S.A.* **1987**, *84*, 7413.
27. Farhood, H.; Serbina, N.; Huang, L. *Biochim. Biophys. Acta* **1995**, *1235*, 289.
28. Zhou, X.; Huang, L. *Biochim. Biophys. Acta* **1994**, *1189*, 195.
29. Litzinger, D. C.; Huang, L. *Biochim. Biophys. Acta* **1992**, *1113*, 201.
30. Mochizuki, S.; Kanegae, N.; Nishina, K.; Kamikawa, Y.; Koiwai, K.; Masunaga, H.; Sakurai, K. *Biochim. Biophys. Acta* **2013**, *1828*, 412.
31. Simmons, J. T.; Allen, J. R.; Morris, D. R.; Clark, R. J.; Levenson, C. W.; Davidson, M. W.; Zhu, L. *Inorg. Chem.* **2013**, *52*, 5838.
32. Keifer, P. A.; Peterkofsky, A.; Wang, G. *Anal. Biochem.* **2004**, *331*, 33.
33. Nogueira, D. R.; Mitjans, M.; Moran, M. C.; Perez, L.; Vinardell, M. P. *Amino Acids* **2012**, *43*, 1203.